



## Triphenyltin degradation and proteomic response by an engineered *Escherichia coli* expressing cytochrome P450 enzyme



Wenying Yi<sup>a</sup>, Kunliang Yang<sup>a</sup>, Jinshao Ye<sup>a,b,\*</sup>, Yan Long<sup>a</sup>, Jing Ke<sup>b</sup>, Huase Ou<sup>a</sup>

<sup>a</sup> Key Laboratory of Environmental Exposure and Health of Guangzhou City, School of Environment, Jinan University, Guangzhou 510632, Guangdong, China

<sup>b</sup> Joint Genome Institute, Lawrence Berkeley National Laboratory, Walnut Creek 94598, CA, USA

### ARTICLE INFO

#### Keywords:

Organotin  
*Bacillus thuringiensis*  
Gene clone  
Proteomics  
ITRAQ

### ABSTRACT

Although triphenyltin (TPT) degradation pathway has been determined, information about the enzyme and protein networks involved was severely limited. To this end, a cytochrome P450 hydroxylase (CYP450) gene from *Bacillus thuringiensis* was cloned and expressed in *Escherichia coli* BL21 (DE3), namely *E. coli* pET32a-CYP450, whose dosage at 1 g L<sup>-1</sup> could degrade 54.6% TPT at 1 mg L<sup>-1</sup> within 6 d through attacking the carbon-tin bonds of TPT by CYP450. Sequence analysis verified that the CYP450 gene had a 1214 bp open reading frame, encoding a protein with 404 amino acids. Proteomic analysis determined that 60 proteins were significantly differentially regulated expression in *E. coli* pET32a-CYP450 after TPT degradation. The up-regulated proteins enriched in a network related to transport, cell division, biosynthesis of amino acids and secondary metabolites, and microbial metabolism in diverse environments. The current findings demonstrated for the first time that P450 received electrons transferring from NADH could effectively cleave carbon-metal bonds.

### 1. Introduction

Bacterial cytochrome P450s belong to the superfamily of proteins with a conserved heme-iron center, catalyzing various molecules as substrates in enzymatic reactions, which made them attractive as potential catalysts for chemical reactions in industries (Grogan, 2011) and environmental remediation. Regarding pollutant degradation, those approved reactions included hydroxylation, oxidation (Ballesteros-Gomez et al., 2015; Frank et al., 2014; Whitehouse et al., 2012), denitrification (Shinkai et al., 2016), sulfoxidation (Renard et al., 2014), N-dealkylation (Roberts et al., 2016), cyclopropanation (Coelho et al., 2013) and intramolecular sp<sup>3</sup> C-H amination (Singh et al., 2014). The metabolism pathways of xenobiotics by cytochrome P450, including benzopyrene, naphthalene, aflatoxin, trichloroethylene, dimethylbenzanthracene, bromobenzene, nitronaphthalene and 1,1-dichloroethylene, have been summarized in the kegg database ([http://www.kegg.jp/dbget-bin/www\\_bget?map00980](http://www.kegg.jp/dbget-bin/www_bget?map00980)). However, the transformation of organometallic compounds with carbon-metal bonds that have characters in between ionic and covalent, and the cleavage of these bonds by P450 are still not clear. The elucidation of these reactions will extend the earlier findings about P450 catalysis, and exhibit insights into the biodegradation of

compounds with carbon-metal bonds.

As an organometallic compound, triphenyltin (TPT) has been extensively used as an active component of herbicides, disinfectants, biocides, antifouling paints and plastic catalysts (Antes et al., 2011; Renard et al., 2014). However, its high toxicity to various invertebrates and vertebrates has been approved, seriously disturbing the endocrine system, preventing enzyme expression and causing reproductive problem (Graceli et al., 2013; Harada et al., 2015; Zuo et al., 2014). Except for its toxicity, the biodegradation of TPT has also been investigated. The results certified that TPT dephenylation was related to the cellular metabolism of ions, carbohydrates and organic acids (Gao et al., 2014). To further reveal the mechanism of TPT degradation by the effective microbes, it is vital to study the response of cellular proteome rather than only focus on the expression of a single effective enzyme because the cellular metabolic pathways associated with TPT degradation are regulated by the entire set of proteins and their networks.

Among the effective microbes selected for TPT degradation, *Bacillus thuringiensis* is a Gram-positive bacterium, commonly used as a biopesticide, which has been proved without negative impact on human, wildlife, pollinators and most other beneficial insects (Lu et al., 2012; Melo et al., 2016). Apart from insect control, *B. thuringiensis* was also used to degrade pollutants, such as dimethyl phthalate (Brar et al.,

\* Corresponding author at: Key Laboratory of Environmental Exposure and Health of Guangzhou City, School of Environment, Jinan University, Guangzhou 510632, Guangdong, China.

E-mail addresses: [jinshaoye@lbi.gov](mailto:jinshaoye@lbi.gov), [folaye@126.com](mailto:folaye@126.com) (J. Ye).

<http://dx.doi.org/10.1016/j.ecoenv.2016.11.012>

Received 3 August 2016; Received in revised form 15 November 2016; Accepted 18 November 2016

Available online 19 December 2016

0147-6513/ © 2016 Elsevier Inc. All rights reserved.

2009), fipronil (Mandal et al., 2013) and TPT (Huang et al., 2014). Metabolite analysis confirmed that TPT was degraded through the cleavage of the Sn-C bonds producing diphenyltin, monophenyltin and tin, respectively (Huang et al., 2014). Based on these degradation products, and the reactions catalyzed by P450 (Arnold, 2015; Ren, et al., 2016) and genomic analysis of *B. thuringiensis*, P450 expressed in this strain was speculated to be the enzyme for TPT degradation.

To prove the above hypothesis, CYP450 gene was cloned and expressed in *Escherichia coli* BL21 (DE3), the recombinant host for CYP450 expression (Biggs et al., 2016; Colthart et al., 2016). The insight into the interaction among P450, cellular proteome and TPT degradation was investigated through an iTRAQ based quantitative proteomic technology.

## 2. Materials and methods

### 2.1. Strains and chemicals

*B. thuringiensis* GIMCC1.817 was an effective strain for TPT degradation (Tang et al., 2016) and was stored at the Microbiology Culture Center of Guangdong Province, China. PUCm-T and pET32a vectors were used for gene cloning and expression, respectively. pET32a-CYP450 was an expression vector containing CYP450. *E. coli* pET32a-CYP450 and *E. coli* pET32a were the expression strains containing CYP450 and an empty plasmid without CYP450, separately. Triphenyltin chloride (purity=98.8%) was obtained from Sigma Aldrich (St. Louis, MO, USA). Lysogeny broth (LB) medium consisted of (in g L<sup>-1</sup>) 10 tryptone, 5 yeast extract and 5 NaCl was used to culture *B. thuringiensis* and *E. coli*. The mineral salt medium (MSM) for TPT degradation contained (in mg L<sup>-1</sup>) 150 Na<sub>2</sub>HPO<sub>4</sub>·12H<sub>2</sub>O, 50 KH<sub>2</sub>PO<sub>4</sub>, 30 NH<sub>4</sub>Cl, 5 Zn(NO<sub>3</sub>)<sub>2</sub> and 5 MgSO<sub>4</sub> (Huang et al., 2014).

### 2.2. Cloning of cytochrome P450 hydroxylase gene

The genomic DNA of *B. thuringiensis* was used as the template for PCR amplification. The coding region of CYP450 gene was amplified by PCR with the specific primers, CYP450F (5'-GGGGGATCCATGGCTTCACCTGAAAAT-3') and CYP450R (5'-CCCCTCGAGTTATTTAGCTTTCAATCGAATAGG-3'), which were designed according to the complete genome of *B. thuringiensis*. PCR was performed at 94 °C for 4 min, followed by 30 cycles at 94 °C for 1 min, 57 °C for 1 min, 72 °C for 1 min, and 72 °C for 10 min as a final extension step by using a thermal cycler. The PCR product was purified, linked to the pUCm-T vector and sequenced. Homology searches of nucleotide sequences were finished by BLAST at NCBI.

### 2.3. Expression of CYP450 gene in *E. coli*

The above PCR product was purified by gel extraction kit, digested with restriction enzymes BamHI and XhoI, and then ligated into pET32a(+) vector which was digested with the same enzymes to form the recombinant expression plasmid pET32a-CYP450. The recombinant vector pET32a-CYP450 was transferred into *E. coli* BL21 (DE3) for protein expression. Meanwhile empty plasmid without CYP450 was also transferred into *E. coli* BL21 (DE3) competent cells. *E. coli* pET32a-CYP450 and *E. coli* pET32a were separately grown at 37 °C in 200 mL LB medium containing 100 mg L<sup>-1</sup> ampicillin at 180 r min<sup>-1</sup>. When the optical density at 600 nm of the medium was about 0.6–0.8, isopropyl-β-D-thiogalactoside was added at a final concentration of 1 mM, and the mixture was further cultured at 37 °C for 4 h. SDS-PAGE was performed using 12.5% separation gel and 4.5% stacking gel. Protein bands were stained with coomassie brilliant blue R-250. Zymogram analysis was performed according to the method used by Lee et al. (2007).

### 2.4. TPT degradation experiments

*E. coli* pET32a-CYP450 and *E. coli* pET32a were inoculated into the culture medium at 37 °C on a rotary shaker at 130 r min<sup>-1</sup>, respectively. After then, the cells were separated from the medium by centrifugation at 3500 g for 10 min and washed three times with sterile distilled water before use in the further experiments. Biodegradation of TPT at 1 mg L<sup>-1</sup> by 1 g L<sup>-1</sup> *E. coli* pET32a-CYP450 or *E. coli* pET32a was performed in 20 mL MSM at 30 °C on a rotary shaker at 130 r min<sup>-1</sup> for 1–6 d. Three samples for each experiment were taken and the mean values were used in calculations. After degradation, 10 mL hexane was added into the MSM. The mixture was sonicated for 20 min in an ultrasonic bath. After the organic phase was collected, 10 mL hexane was added into the aqueous phase to extract TPT again. The collected organic part was concentrated using a rotary evaporator at 30 °C. Subsequently, the residues were dissolved by 5 mL methanol and derivatized in pH 4.5 acetate buffer with 2 mL of 2% sodium diethyl dithiocarbonate. TPT was analyzed according to previously published methods (Ye et al., 2013) by gas chromatography-mass spectrometry (GC-MS, 7890/5975 C, Agilent Technologies, Santa Clara, CA, USA) equipped with an Rxi-5MS GC column (30 m × 0.25 mm × 0.25 μm). Briefly, helium at 1.1 mL min<sup>-1</sup> was used as the carrier gas. The column temperature program started at 50 °C for 1.5 min. Subsequently, the oven was heated to 300 °C at an efficiency of 10 °C min<sup>-1</sup> for 4 min. The solvent cut time was set to 2.6 min. Mass spectra were recorded at 1 scan s<sup>-1</sup> under electronic impact with electron energy of 70 eV, and mass ranged 55–650 atoms to mass unit. The detection limit of TPT was 250 ng L<sup>-1</sup>.

### 2.5. Protein preparation and digestion

The cells of *E. coli* pET32a-CYP450 before and after degradation were suspended in 1 mL lysis buffer added with 0.2 g L<sup>-1</sup> phenylmethylsulfonyl fluoride, 2% v/v IPG buffer and 0.6 g L<sup>-1</sup> DTT (Ou, et al., 2017). The samples were frozen in liquid nitrogen thrice for 15 min per time, and subsequently treated by ultrasonication for 20 min. Nuclease was added to the lysate at a final concentration of 1% v/v. After the mixture was incubated at 4 °C for 30 min, the cell debris was removed at 4 °C by centrifugation at 13500 g for 1 h. The resultant proteins from each sample were reduced by 10 mM DTT for 1 h at 37 °C, and blocked with 1 μL cysteine blocking reagent for 10 min at room temperature. Subsequently, the samples were added in 10 KD Amicon Ultra-0.5 centrifugal filter devices, and centrifuged at 12000 g for 20 min. The proteins in filter devices were digested by 50 μL trypsin (Promega, V5280, USA) at 4% w/w overnight at 37 °C. After centrifugation, 1 μg trypsin was added to each filter for 2 h. The concentration of tryptic peptides in the liquid collection tube was measured using the Bradford method.

### 2.6. iTRAQ labeling and desalination

Tryptic peptides were labeled with an iTRAQ reagent multiplex kit (Sigma, PN 4352135, USA) according to the manufacturer's instructions. Briefly, the contents of an iTRAQ® Reagent vial was transferred to a sample tube, and incubated at room temperature for 1 h. Subsequently, 100 μL water was added to each sample to stop the reaction. After determination of the labeling efficiency by ABI 4800 MALDI TOF/TOF mass spectrometer (Applied Biosystems, Foster City, CA), the iTRAQ-labeled samples were mixed, centrifuged, desalinated with Strata-X (Phenomenex, USA), separated by strong cation exchange chromatography (SCX), and dried in a vacuum concentrator, respectively. The samples were then resolved with solution (2% v/v acetonitrile, 0.1% v/v formic acid), centrifuged at 12000 r min<sup>-1</sup> for 20 min and detected by an AB SCIEX Triple TOF 5600 mass spectrometer (AB SCIEX, Framingham, MA, USA) equipped with a Nanospray III source (AB SCIEX) using the following parameter settings (Cui et al., 2015): spray voltage, 2.3 kV; sheath gas (nitrogen) pressure, 30 psi; collision

gas (argon) pressure, 15 psi; vaporizer temperature, 120 °C. Survey scans were acquired in 250 ms, and up to 30 product ion scans were collected if they exceeded a threshold of 120 counts per second (counts/s) with a 2+–5+ charge-state. A sweeping collision energy setting of  $35 \pm 5$  eV coupled with iTRAQ adjusted rolling collision energy was applied to all precursor ions for collision-induced dissociation. Dynamic exclusion was set for half of the peak width (18 s), and the precursor was then refreshed off the exclusion list.

### 2.7. Bioinformatics analysis

Proteins were searched and analyzed using SWISS-Prot Protein Database (<http://www.expasy.ch/ch2d/>). Identified proteins were screened by fault occurrence rate or unused value to select reliable proteins whose confidence was higher than 99% for further analysis. Proteins with at least a 1.2-fold increase or decrease were determined as the significantly differential expression proteins. Biological process, molecular function and cellular component of the identified proteins were annotated by searching the PANTHER classification database (<http://www.pantherdb.org/>). The protein-protein networks of significantly differentially expressed proteins were analyzed by STRING software (<http://www.string-db.org/>).

## 3. Results and discussion

### 3.1. Gene cloning and sequence analysis of CYP450 from *B. thuringiensis*

The full length coding region of CYP450 gene had an open reading frame of 1214 bp, encoding a protein with a theoretical molecular mass (MW) of 46.87 kDa and a theoretical isoelectric point of 5.57. This expressed protein with totally 404 amino acid residues included 62 acidic amino acids (D, E), 52 alkaline amino acids (K, R), 96 polar amino acids (N, C, Q, S, T, Y), 148 hydrophobic amino acids (A, I, L, F, W, V) and other kinds of amino acid residues.

Sequence alignments at NCBI database (<http://www.ncbi.nlm.nih.gov/>) showed that the amino acid sequence of CYP450 gene in the current study had higher homology with those in other bacteria, such as *Bacillus cereus* (Fig. S1, Supplementary data). Since it contained some conserved motifs as the proved CYP450s, the current CYP450 might exhibit the similar molecular functions as them, which also indicated that the understanding of the chemical bond cleavage and generation triggered by the present CYP450 would exhibit some novel insights into the functions of this superfamily of proteins. That was one of the reasons why CYP450 was selected in the present study as a potential enzyme to degrade TPT, whose molecular structure was similar to aromatic compounds containing benzene rings but also with unique carbon-tin bonds. Metabolite analysis in our previous studies has confirmed that TPT was degraded through the successive dephenylation pathway by *B. thuringiensis* (Tang et al., 2016). If direct evidence could be provided that the reactions involved were catalyzed by CYP450, it would be the first time to confirm that CYP450 can cleave carbon-metal bonds, which means that it can be used to transform organometallic pollutants.

### 3.2. CYP450 expression

SDS-PAGE analysis confirmed the expression of CYP450 in *E. coli* after isopropyl- $\beta$ -D-thiogalactoside induction (Fig. 1A). Compared with *E. coli* pET32a, *E. coli* pET32a-CYP450 exhibited an obvious protein band at about 65 kDa with the 20 kDa pET32a plasmid vector. It could be calculated that the MW of CYP450 was about 45 kDa, which was consistent with the theoretical MW of 46.87 kDa. Meanwhile, no protein band at this MW was observed in the *E. coli* pET32a, which illustrated that this strain did not contain CYP450. Zymogram analysis found a protein peak ( $m/z$  1813.833, Fig. 1B) after the protein in monolithic gel was digested by protease. The results searched at SWISS-

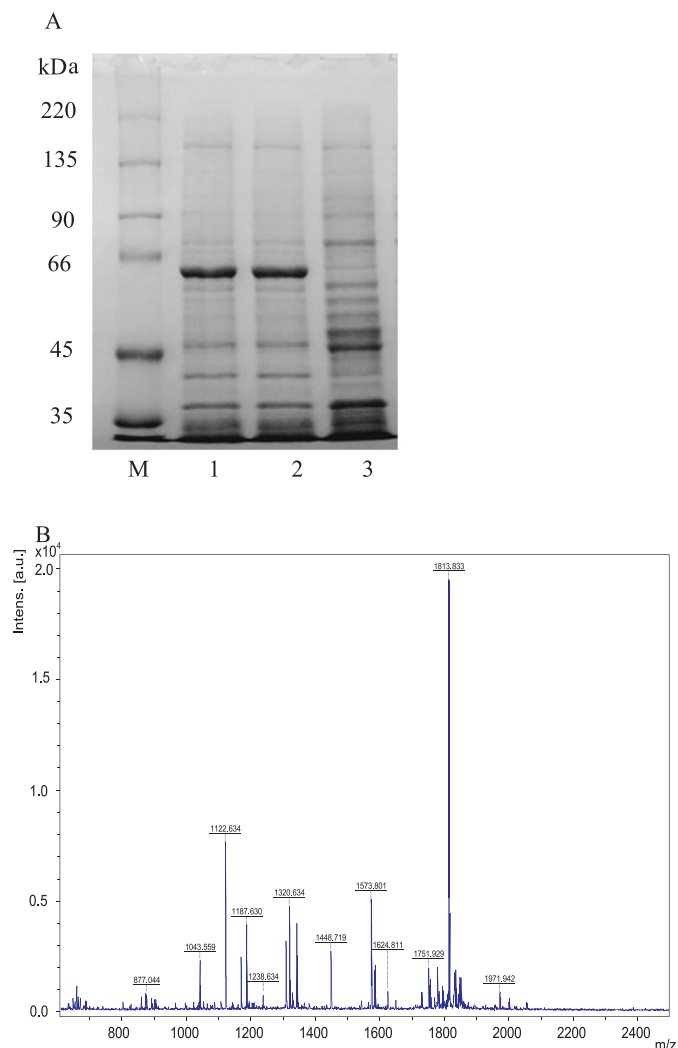


Fig. 1. (A) SDS-PAGE analysis of CYP450 from *B. thuringiensis* expressed in *E. coli*. Lanes M, 1, 2 and 3 stand for low molecular weight protein standards, crude enzymes extracted from *E. coli* pET32a-CYP450, *E. coli* pET32a-CYP450 and *E. coli* pET32a, respectively; and (B) Zymogram analysis of CYP450.

Prot Protein Database (<http://www.expasy.ch/ch2d/>) further confirmed that protein with  $m/z$  at 1813.833 was cytochrome P450 hydroxylase, proving P450 from *B. thuringiensis* has been expressed in *E. coli* BL21 (DE3) successfully.

### 3.3. TPT degradation

The TPT degradation by *E. coli* pET32a-CYP450 was significantly higher than by *E. coli* pET32a (Fig. 2A), which confirmed that CYP450 was TPT degradation enzyme. The degradation efficiency of TPT at  $1 \text{ mg L}^{-1}$  by  $1 \text{ g L}^{-1}$  of *E. coli* pET32a-CYP450 was up to about 54.6% at 6 d (Fig. 2A). Regarding the degradation pathway, metabolite analysis has been verified that TPT was transformed primarily through the cleavage of the carbon-tin bonds (Huang et al., 2014), whereas, the bond energy and molecular properties of TPT computed by ChemBio3D Ultra indicated that hydroxylation occurred in C(4) of the tin-linked benzenes of TPT was also a potential way for TPT degradation (Tang et al., 2016).

Based on these published results, and TPT molecular structure and P450 bioinformatics, the potential TPT degradation pathways were further revealed (Fig. 2B). The primary pathway of TPT transformation was that the tin atom of TPT was bound to the heme center of P450, inducing a change in the protein conformation and receiving an



and DnaK) (Arita-Morioka et al., 2015), biosynthesis of amino acids (Prs, Pkg, GapA, AroB, TrpC and TrpA) (Juminaga et al., 2012) and secondary metabolites (Prs, Pkg, GapA, AroB, TrpC, TrpA and Acs), and microbial metabolism in diverse environments (Prs, Pkg, GapA, GhrA, YdbK and Acs). Although some metabolites, such as diphenyltin and monophenyltin (Tang et al., 2016), generated in the TPT degradation process might pose some inhibitive effects on *E. coli* pET32a-CYP450, triggering the up expression of some proteins involved in the cellular adaptation in a diverse environment, the biosynthesis of amino acids and proteins, and even the growth of cells were significantly improved. However, the down regulation network mainly related to oxidative phosphorylation (Haussmann et al., 2012) and CoA synthesis did not enrich enough proteins to a significant number (Fig. 3C), meaning that TPT degradation did not exhibit a significant depressed impact on cellular metabolism at a protein network level.

To further verify the proteome response during the TPT degradation process, the specific functions of some biomarkers and key note proteins were annotated. Among these proteins, the up-regulated synthesis NAD(P) transhydrogenase subunit beta (PntB) responsible for transhydrogenation between NAD(P)H and NAD(P)<sup>+</sup> was a biomarker directly related to TPT degradation catalyzed by P450 in the current study. P450s are the terminal oxidase enzymes in the electron transfer chain, accepting electrons delivered from NAD(P)H after substrate binding by the cysteine-iron active site, which resulted in the catalysis of a variety of reactions. To eliminate damaged proteins induced by various stresses through misfolding and aggregation, a heat-shock response network was developed during the bacterial evolution process (Fuhrmann et al., 2009). The coexistence and up regulation of the small heat shock proteins (IbpA and IbpB) and ATP-dependent chaperone protein (DnaK) assisted the folding and assembly of proteins with functionally active conformations in the recombinant strain *E. coli* pET32a-CYP450 during the TPT degradation process. The up regulation of these proteins responsible for stress response illustrated that the degradation intermediates, including diphenyltin and monophenyltin, did pose some stresses to *E. coli* pET32a-CYP450. However, the inhibitive effect was not significant at protein network level (Fig. 3C).

Three subunits of ATP synthase, ATP synthase subunit beta (AtpD) and ATP synthase gamma chains (AtpA and AtpG), involved in energy metabolism were significantly up regulated expression. ATP synthases are the membrane-bound proteins derived energy from proton motive force by rotary catalysis and transferred it to adenosine diphosphates (ADP) to constitute ATP molecules (Allegretti et al., 2015). Furthermore, the up regulation of the energy related proteins appeared to be a common effect during the xenobiotic biodegradation process (Szewczyk et al., 2015). In this study, the up-regulation expression of these three subunits of ATP synthase suggested high energy demands of *E. coli* pET32a-CYP450 during the TPT degradation process.

### 3.5. Pathway analysis of the differentially expressed proteins

To determine the relation between the differentially expressed proteins and metabolism pathways during the TPT degradation process, the KEGG pathways that were regulated by the differentially expressed proteins were summarized and shown in Fig. 4. The biomarkers PflB, GapA, AcsA, FrmA, Pkg, AroB, TrpC and TrpA were enriched in glycolysis/gluconeogenesis, pyruvate metabolism, phenylalanine, tyrosine and tryptophan biosynthesis, and pantothenate and CoA biosynthesis pathways. Carbohydrate metabolic pathway and amino acid metabolism pathway were obviously activated, whereas, pantothenate and CoA biosynthesis pathway was inhibited.

Three proteins phosphoglycerate kinase (Pkg), S- (hydroxymethyl) glutathione dehydrogenase (FrmA) and glyceraldehyde 3-phosphate dehydrogenase A (GapA) related to glycolysis pathway were up-regulated expressed, which verified that more energy were generated in the carbohydrate metabolism pathway by *E. coli* pET32a-CYP450 for TPT degradation. This finding is consistent with the up-regulated

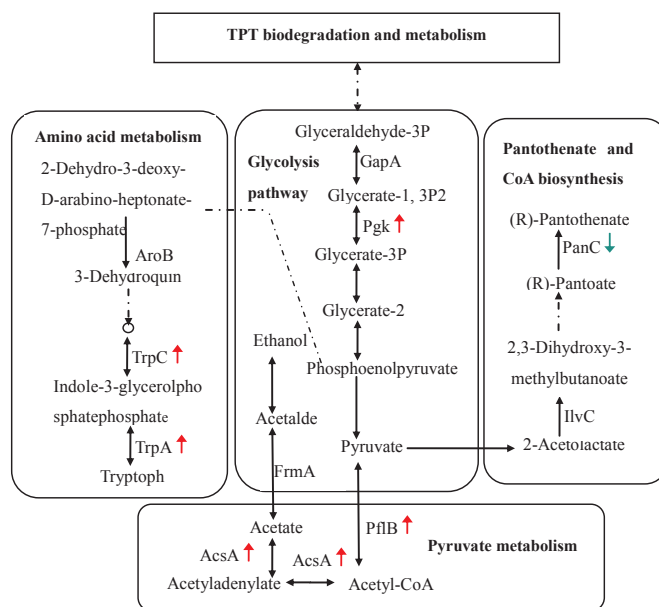


Fig. 4. KEGG pathway analysis of the differentially expressed proteins. ↑ arrows represent up-regulated synthesis and ↓ arrows stand for down-regulated expression.

biosynthesis of AtpA, AtpD and AtpG, and the vigorous energy metabolism controlled by these three ATPases. The protein, GapA was widely known as a glycolytic enzyme catalyzing the conversion of glyceraldehyde 3-phosphate to 3-phospho-D-glyceroyl phosphate coupled with the reduction of NAD<sup>+</sup> to NADH (Freitag et al., 2012), which is in agreement with the up regulation of PntB and the enhancement of electron transfer from NADH to P450 during the TPT degradation process.

Regarding Pkg, it involved the conversion of ADP and 3-phospho-D-glyceroyl phosphate to ATP and 3-phospho-D-glycerate leading to energy synthesis. The up-regulation of Acs and PflB related to pyruvate metabolism was also confirmed the improvement of energy synthesis, offering more energy and electrons to P450 for TPT transformation.

The enhanced synthesis of AroB (Karki and Ham, 2014), TrpC and TrpA associated with phenylalanine, tyrosine and tryptophan biosynthesis (Molina-Henares et al., 2009) confirmed that amino acid metabolism was the significantly regulated metabolism pathway during the TPT degradation process. As for AroB, it catalyzed the conversion of 3-deoxy-D-arabino-heptulosonate 7-phosphate into 3-dehydroquinate and phosphate. Regarding TrpC, it participated in degradation of 1-(2-carboxyphenylamino)-1-deoxy-D-ribose5-phosphate with releasing CO<sub>2</sub> and generating 1-C-(3-indolyl)-glycerol 3-phosphate. In addition, TrpA (Fuller et al., 2016), a protein capable of converting L-serine and 1-C-(indol-3-yl)glycerol 3-phosphate to L-tryptophan.

The synthesis of ketol-acid reductoisomerase (IlvC) and pantothenate synthetase (PanC) related to pantothenate and CoA biosynthesis was decreased. IlvC catalyzed the conversion of 2-acetylactate into 2,3-dihydroxy-3-methylbutanoate with the consumption of NADPH. PanC was an enzyme involved in the last step of pantothenate biosynthesis, and responsible for reducing pantoate and β-alanine to form pantothenate with the consumption of ATP. Because most reactions of the amino acid, glycolysis and CoA biosynthesis networks are reversible, the inhibition of the pantothenate and CoA biosynthesis pathway meant that this network was acted as a source for glycolysis and amino acid metabolism (Freitag et al., 2012), generating energy and target proteins for TPT degradation.

## 4. Conclusions

The cytochrome P450 hydroxylase gene from *B. thuringiensis* was successfully cloned and expressed in *E. coli*, which could degrade 54.6%

of TPT at 1 mg L<sup>-1</sup> within 6 d. P450 received electrons transferred from NADH, and attacked carbon-tin bonds of TPT, triggering its degradation. During this process, the carbohydrate metabolism, energy metabolic pathway and amino acid metabolism in *E. coli* pET32a-CYP450 were enhanced, whereas, pantothenate and CoA biosynthesis pathway was inhibited. These findings exhibited insights into carbon-metal bonds cleavage catalyzed by P450, and the protein networks involved.

## Acknowledgements

The authors would like to thank the National Natural Science Foundation of China (Nos. 21377047, 21577049), Science and Technology Planning Project of Guangdong Province, China (Nos. 2014A020216013, 2016A020222005) for their financial support.

## Appendix A. Supplementary material

Supplementary data associated with this article can be found in the online version at doi:10.1016/j.ecoenv.2016.11.012.

## References

- Allegretti, M., et al., 2015. Horizontal membrane-intrinsic alpha-helices in the stator a-subunit of an F-type ATP synthase. *Nature* 521, 237–240.
- Antes, F.G., et al., 2011. Speciation and degradation of triphenyltin in typical paddy fields and its uptake into rice plants. *Environ. Sci. Technol.* 45, 10524–10530.
- Arita-Morioka, K., et al., 2015. Novel strategy for biofilm inhibition by using small molecules targeting molecular chaperone DnaK. *Antimicrob. Agents* 59, 633–641.
- Arnold, F.H., 2015. The nature of chemical innovation: new enzymes by evolution. *Q. Rev. Biophys.* 48, 404–410.
- Ballesteros-Gomez, A., et al., 2015. In vitro human metabolism of the flame retardant resorcinol bis(diphenylphosphate) (RDP). *Environ. Sci. Technol.* 49, 3897–3904.
- Biggs, B.W., et al., 2016. Overcoming heterologous protein interdependency to optimize P450-mediated taxol precursor synthesis in *Escherichia coli*. *Proc. Natl. Acad. Sci. USA* 113, 3209–3214.
- Brar, S.K., et al., 2009. Concurrent degradation of dimethyl phthalate (DMP) during production of *Bacillus thuringiensis* based biopesticides. *J. Hazard. Mater.* 171, 1016–1023.
- Coelho, P.S., et al., 2013. Olefin cyclopropanation via carbene transfer catalyzed by engineered cytochrome P450 enzymes. *Science* 339, 307–310.
- Colthart, A.M., et al., 2016. Detection of substrate-dependent conformational changes in the P450 fold by nuclear magnetic resonance. *Sci. Rep.* 6, 22035.
- Cui, R., et al., 2015. Proteomic analysis of cell proliferation in a human hepatic cell line (HL-7702) induced by perfluorooctane sulfonate using iTRAQ. *J. Hazard. Mater.* 299, 361–370.
- Frank, D.J., et al., 2014. Cholesterol ester oxidation by mycobacterial cytochrome P450. *J. Biol. Chem.* 289, 30417–30425.
- Freitag, J., et al., 2012. Cryptic peroxisomal targeting via alternative splicing and stop codon read-through in fungi. *Nature* 485, (522-U135).
- Fuhrmann, J., et al., 2009. McsB is a protein arginine kinase that phosphorylates and inhibits the heat-shock regulator CtsR. *Science* 324, 1323–1327.
- Fuller, J.J., et al., 2016. Biosynthesis of violacein, structure and function of L-tryptophan oxidase VioA from *Chromobacterium violaceum*. *J. Biol. Chem.* 291, 20068–20084.
- Gao, J., et al., 2014. Biosorption and biodegradation of triphenyltin by *Stenotrophomonas maltophilia* and their influence on cellular metabolism. *J. Hazard. Mater.* 276, 112–119.
- Graceli, J.B., et al., 2013. Organotin: a review of their reproductive toxicity, biochemistry, and environmental fate. *Reprod. Toxicol.* 36, 40–52.
- Grogan, G., 2011. Cytochromes P450: exploiting diversity and enabling application as biocatalysts. *Curr. Opin. Chem. Biol.* 15, 241–248.
- Guengerich, F.P., Munro, A.W., 2013. Unusual cytochrome P450 enzymes and reactions. *J. Biol. Chem.* 288, 17065–17073.
- Harada, S., et al., 2015. Structural basis for PPAR gamma transactivation by endocrine-disrupting organotin compounds. *Sci. Rep.* 5, 8520.
- Hausmann, U., et al., 2012. Global proteome survey of protocatechuate- and glucose-grown *Corynebacterium glutamicum* reveals multiple physiological differences. *J. Proteom.* 75, 2649–2659.
- Huang, J., et al., 2014. Triphenyltin biosorption, dephenylation pathway and cellular responses during triphenyltin biodegradation by *Bacillus thuringiensis* and tea saponin. *Chem. Eng. J.* 249, 167–173.
- Juminaga, D., et al., 2012. Modular engineering of L-tyrosine production in *Escherichia coli*. *Appl. Environ. Microbiol.* 78, 89–98.
- Karki, H.S., Ham, J.H., 2014. The roles of the shikimate pathway genes, *aroA* and *aroB*, in virulence, growth and UV tolerance of *Burkholderia glumae* strain 411gr-6. *Mol. Plant Pathol.* 15, 940–947.
- Lee, Y.S., et al., 2007. Cloning, purification, and characterization of chitinase from *Bacillus* sp DAU101. *Bioresour. Technol.* 98, 2734–2741.
- Lu, Y.H., et al., 2012. Widespread adoption of Bt cotton and insecticide decrease promotes biocontrol services. *Nature* 487, 362–365.
- Mandal, K., et al., 2013. Microbial degradation of fipronil by *Bacillus thuringiensis*. *Ecotox. Environ. Safe* 93, 87–92.
- Melo, A.L.D., et al., 2016. *Bacillus thuringiensis*: mechanism of action, resistance, and new applications: a review. *Crit. Rev. Biotechnol.* 36, 317–326.
- Molina-Henares, M.A., et al., 2009. Functional analysis of aromatic biosynthetic pathways in *Pseudomonas putida* KT2440. *Microb. Biotechnol.* 2, 91–100.
- Ou, H.S., et al., 2017. Degradation of tris(2-chloroethyl) phosphate by ultraviolet-persulfate: kinetics, pathway and intermediate impact on proteome of *Escherichia coli*. *Chem. Eng. J.* 308, 386–395.
- Renard, L., et al., 2014. Hybrid organotin and tin oxide-based thin films processed from alkynylorganotin: synthesis, characterization, and gas sensing properties. *ACS Appl. Mater. Interfaces* 6, 17093–17101.
- Ren, X.K., et al., 2016. Synthesis of imidazolidin-4-ones via a cytochrome P450-catalyzed intramolecular C–H amination. *ACS Catal.* 6, 6833–6837.
- Roberts, A.G., et al., 2016. The role of cytochrome P450 BM3 phenylalanine-87 and threonine-268 in binding organic hydroperoxides. *Biochim. Biophys. Acta* 1860, 669–677.
- Shinkai, Y., et al., 2016. NADPH-cytochrome P450 reductase-mediated denitration reaction of 2,4,6-trinitrotoluene to yield nitrite in mammals. *Free Radic. Biol. Med.* 91, 178–187.
- Singh, R., et al., 2014. P450-catalyzed intramolecular C-H amination with arylsulfonyl azide substrates. *ACS Catal.* 4, 546–552.
- Szewczyk, R., et al., 2015. Mechanism study of alachlor biodegradation by *Paecilomyces marquandii* with proteomic and metabolomic methods. *J. Hazard. Mater.* 291, 52–64.
- Tang, L., et al., 2016. Correlation among phenyltins molecular properties, degradation and cellular influences on *Bacillus thuringiensis* in the presence of biosurfactant. *Biochem. Eng. J.* 105, 71–79.
- Tripathi, S., et al., 2013. Structural basis for effector control and redox partner recognition in cytochrome P450. *Science* 340, 1227–1230.
- Urlacher, V.B., Girhard, M., 2012. Cytochrome P450 monooxygenases: an update on perspectives for synthetic application. *Trends Biotechnol.* 30, 26–36.
- Wang, Z.J., et al., 2014. Cytochrome P450-catalyzed insertion of carbenoids into N-H bonds. *Chem. Sci.* 5, 598–601.
- Whitehouse, C.J., et al., 2012. P450(BM3) (CYP102A1): connecting the dots. *Chem. Soc. Rev.* 41, 1218–1260.
- Ye, J., et al., 2013. Biosorption and biodegradation of triphenyltin by *Brevibacillus brevis*. *Bioresour. Technol.* 129, 236–241.
- Yosca, T.H., et al., 2013. Iron(IV)hydroxide pK(a) and the role of thiolate ligation in C-H bond activation by cytochrome P450. *Science* 342, 825–829.
- Zuo, Z.H., et al., 2014. Chronic exposure to tributyltin chloride induces pancreatic islet cell apoptosis and disrupts glucose homeostasis in male mice. *Environ. Sci. Technol.* 48, 5179–5186.